

# Catastrophic failure of outbreak containment: Limited testing causes discontinuity in epidemic transition

Davide Scarselli,\* Nazmi Burak Budanur,\* and Björn Hof

*IST Austria, 3400 Klosterneuburg, Austria*

(Dated: January 5, 2022)

Standard measures such as quarantining suspects and contact tracing could not contain the ongoing COVID-19 pandemic. Unlike for other recent epidemics where such instruments were successful, in the present case a large fraction of the infected have only mild unspecific symptoms. By employing network models we here show that even for near perfect contact tracing and unlimited suspect testing, containment starts to fail when more than approximately half of the carriers fall into the weak-symptom category. The situation becomes considerably more severe if the number of daily available tests is limited. In this case the epidemic transition becomes discontinuous and a much larger percentage of the population becomes infected. While moderate levels of social distancing can bring the situation back under control, the limited number of daily tests introduces a finite time horizon: If social distancing is implemented after the cut off date, containment catastrophically breaks down resulting in an exponential disease spread.

## I. INTRODUCTION

Suspect testing combined with quarantining and contact tracing have been key in slowing the spread of COVID-19. However, unlike for the 2002–2004 SARS outbreak and the 2013–2016 Western African Ebola virus epidemic, this containment strategy did not suffice to stop the present pandemic. A key difference to these earlier cases is that approximately 80% of the COVID-19 infections appear to be mild, and some studies even suggest that approximately 50% of the total cases are symptom free [1–4]. Various studies have reported evidence of transmission by weak-symptom carriers [2, 5] and patient tests conducted with symptomatic and asymptomatic patients indicated comparable viral loads in both categories [6]. It is evident that transmission by carriers that are either asymptomatic or only have weak unspecific symptoms, poses a severe obstacle to containment. However, even carriers without symptoms can be detected if traced as a contact of a symptomatic person. Hence the ratio of symptomatic to weak-symptom carriers as well as the efficiency of contact identification are key factors that decide if eventually a disease will spread

---

\* These two authors contributed equally

exponentially or can be contained.

Using network models in the following, we address the question whether suspect testing and high efficiency contact tracing can contain epidemics with varying ratios of weak-symptom carriers. As will be shown for epidemics with spreading rates comparable to that of COVID-19, if more than half of the carriers have weak symptoms the disease cannot be contained by these standard procedures alone. If aided by social distancing (SD) containment can be achieved but crucially SD must be implemented early on. If SD is introduced even marginally too late, testing is overwhelmed and containment breaks down.

## II. MODEL

We consider an extension of a spatial SEIR (Susceptible-Exposed-Infectious-Recovered) model [7], where each tile on a 2D grid represents an individual which can fall into one of the above four compartments. In addition, infectious are split into two categories, symptomatic ( $I_S$ ) and weak-symptom cases ( $I_W$ ), where the latter ranges from people who may have unspecific symptoms (e.g. coughing) to entirely asymptomatic. As a result of intervention measures, the individuals in states  $S$ ,  $E$  and  $I$  can be put under quarantine, formally increasing the number of possible states to eight, and all possible transition paths are shown in Fig. 1 (a) (see caption for details). The key features of the model (see also [7]) can be understood from the example given in Fig. 1 (b). An infectious individual with weak symptoms (brown tile bottom right of Fig. 1 (b)) can at each time step transmit the disease with a given probability to each of the four nearest neighbours, plus to a randomly chosen distant individual (mimicking encounters during shopping, travel etc.) with the same probability, if the target is susceptible. Moreover, we assume that weak-symptom individuals do not raise suspicion and continue to spread the disease. This is in particular likely when other infections (e.g. flu or common cold) coincide with the epidemic. A strongly symptomatic case (red tile in Fig. 1 (b)) on the other hand is identified and quarantined (blue dashed box) immediately. After testing positive, its four nearest neighbours are quarantined and queued for testing. For every new positive case, the quarantining and testing procedure is continued. In this idealized setting, testing therefore eradicates local clusters with perfect efficiency. However, random encounters with distant individuals are generally much harder to track and, for simplicity, we assume that they remain undetected. As we will show below, this choice of probabilities is particularly suited to understand key features of the epidemic transition in the presence of containment measures. However, none of the findings presented are specific to the parameter choice (e.g. distant encounters

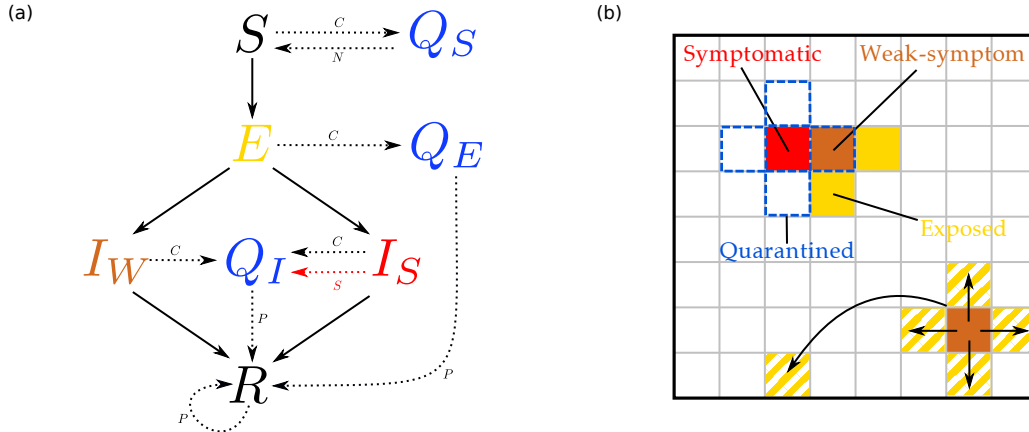


FIG. 1. (a) Transitions between possible states. Solid arrows denote the typical disease progression for an undetected individual, while dotted arrows denote possible events in a quarantining and testing scenario. In particular,  $S$ ,  $E$ ,  $I_W$  and  $I_S$  are quarantined if they are in contact with a known positive (arrow  $C$ ), while  $I_S$  can be immediately identified and quarantined (arrow  $S$ ). After testing negative  $Q_S$  reverts to  $S$  (arrow  $N$ ) while  $Q_E$ ,  $Q_I$  and  $R$  test positive and transform into  $R$ . (b) Spatial implementation. Every day an infectious individual interacts with their neighbours and a randomly selected individual, and transmits the disease with a constant probability if the individuals they interact with are susceptible. Upon identification of a positive case (in figure  $I_S$ ) all the neighbours are put into quarantine and tested. Weak-symptom cases can only be identified if they are neighbours of a known positive case.

can be made traceable etc.). Further robustness tests conducted include simulations with three variants of the basic network model. In the first, we alter the nature of distant encounters to realize a small world network (Kleinberg network, see [8] for details). In the second we introduce high connectivity hubs up to 100 connections. For the third implementation the lattice is removed and the network is scale-free up to a maximum of 100 connections (see [9] for details).

Simulations start from a small group of weak-symptom cases that are randomly scattered across the grid and evolve in a domain representing a population of  $P = 3000 \times 3000$ . We model the incubation and infectious period with a Gamma distribution with unitary scale parameter and mean of 3 and 4 days, respectively (the epidemiological parameters are similar to the ones reported for COVID-19, cf. [10]). The transmission probability is set to 0.38 to reproduce the average growth rate  $\sim e^{0.3[\text{days}^{-1}]t}$  observed during the early exponential phase of the ongoing COVID-19 pandemic.

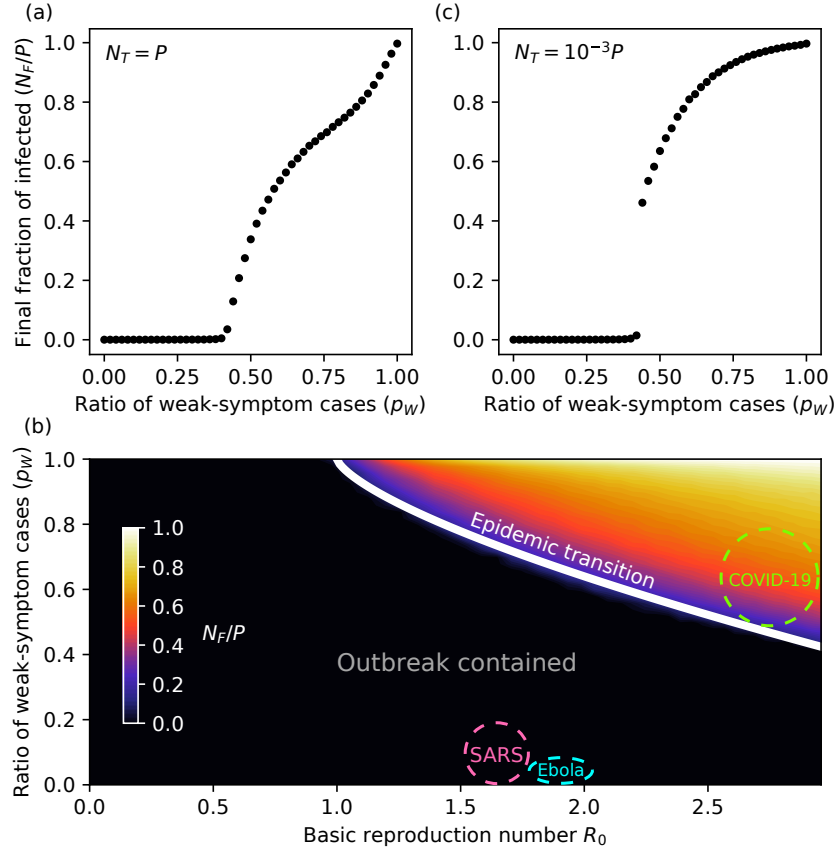


FIG. 2. Containment breakdown driven by weak-symptom carriers. (a) and (b) Final infected fraction of the population ( $N_f/P$ ) as a function of the ratio of weak-symptom cases ( $p_w$ ) for unlimited and limited available daily tests,  $N_T = P$  and  $N_T = 10^{-3}P$ , respectively. When weak-symptom cases appear with less than approximately 40% frequency, outbreaks can be contained efficiently by testing and quarantining. For larger fractions of weak-symptom cases, the disease can not be contained and a large fraction of the population is infected. Limited availability in tests further aggravates the scenario and results in an abrupt transition. (c) Admissible epidemiological parameters that allow successful outbreak containment. Each point of the plot measures the final fraction of infected  $N_f/P$  (cf. colorbar) under unlimited testing conditions ( $N_T = P$ ).  $R_0$  is the basic reproduction number and is computed following [7]. The white line separates epidemics that can be successfully contained and shows that containing outbreaks with a high percentage of weak-symptom infectious cases necessarily requires to lower the basic reproduction number. The approximate parameters of recent epidemics are indicated by dashed circles.

### III. RESULTS

For the first simulation we choose to vary the ratio of weak-symptom carriers (see Fig. 2 (a)). Each data point can be thought of as a different disease where all the other parameters are held constant. Plotted is the ratio of the final infected to the total population  $P$ . In this simulation we

assume that there are always sufficient tests available for all suspects with strong symptoms and for contact tracing. We assume, however, that there are no surplus test capacities, e.g. random checks on high risk groups etc. While such additional testing can greatly enhance containment, during the early phase of the COVID-19 outbreak countries were fully occupied with suspect testing and even strong symptomatic cases had to be put on waiting lists.

As shown in Fig. 2 (a) testing and contact tracing can readily contain the disease when approximately 60% or more of the infected have recognizable symptoms. In contrast, when weak-symptom carriers are above a threshold of approximately 40% an epidemic transition (i.e. a second order phase transition) occurs. Above this threshold a non-vanishing fraction (in the thermodynamic limit) of the population catches the disease. Therefore, even if contact tracing and hence local cluster elimination works to perfection, the disease cannot be contained if the fraction of carriers is above critical. Fig. 2 (b) shows how the critical threshold of weak-symptom carriers scales with the basic reproduction number ( $R_0$ ) of the uncontrolled disease. Estimates for the respective parameters for SARS [11, 12] and Ebola [13–15] show that both of these fall into the category that can be contained by a standard response, while COVID-19 likely does not.

Next, we limit the number of suspects tested per day ( $N_T$ ) to a maximum of 0.1% of the population (i.e. 9000 cases). This percentage is considerably larger than the daily test numbers carried out in any country during the early stages of the COVID-19 epidemic [16], in particular when taking into account that in the model each suspect only requires a single test, whereas in practice individuals had to be tested multiple times [16]. As shown in Fig. 2 (c) limiting testing fundamentally changes the epidemic transition and causes a jump directly above the epidemic threshold to 40% of the population infected. Comparing Fig. 2 (a) and (c), if 50% of the infectious have weak symptoms, for limited tests 65% of the population become eventually infected whereas for unlimited tests this value is only 35%. The abrupt jump in the epidemic transition has been verified for various other settings, including the aforementioned alternative network implementations (see Fig. 3) and different domain sizes (see Fig. 4). Even though the network connectivity slightly shifts the epidemic transition point, in all cases it remains in the range of 35 to 50 percent weak-symptom carriers and moreover all qualitative features are unaffected.

In the following we set the ratio of weak-symptom carriers to 45% (for COVID-19 some studies suggest that asymptomatic cases alone already account for 40% to 50%). Even in this conservative scenario the society is above the epidemic threshold and although slowed down by testing ( $N_T = 10^{-3}P$ ), the disease is not contained and will spread at an exponential rate. However, if in addition social distancing measures are implemented, the spread can be stopped. In the model we assumed

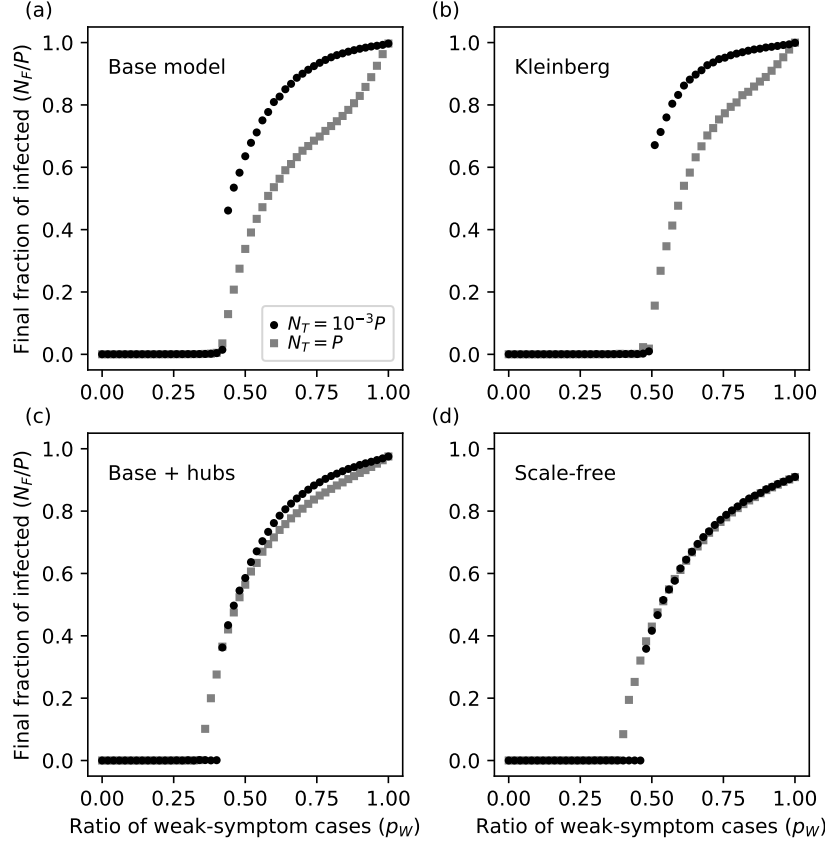


FIG. 3. Effect of the network structure on the transition for unlimited daily tests ( $N_T = P$ , grey dots) and limited daily tests ( $N_T = 10^{-3}P$ , black dots). (a) Base model with population  $P = 3000 \times 3000$ . (b) Kleinberg Navigable Small World Network [8], as implemented in NetworkX 2.4 Python library [17], for a population  $P = 500 \times 500$ . (c) Base model with the addition of high-connectivity hubs for a population  $P = 1000 \times 1000$ . In addition to the local neighbourhood, each individual is assigned a number of random long-range connections sampled from a discrete power-law distribution with exponent 2 and cut-off threshold of 100 connections. (d) Scale-free network (cf. [9]) for a population  $P = 1000 \times 1000$ . Each individual is assigned a number of random connections sampled from a discrete power-law distribution with exponent 2 and cut-off threshold of 100 connections, without a local neighbourhood. In (a) and (b) the domain is initially seeded with  $4 \cdot 10^{-5}P$  randomly scattered weak-symptom cases, whereas in (c) and (d) with  $1 \cdot 10^{-5}P$  randomly scattered weak-symptom cases.

that SD cuts the transmission probability by 15% (the exact value is not important). Interestingly and as shown in Fig. 5 (a) and (b), SD must be implemented early and if introduced after a cut off day containment breaks down and the fraction of the population finally infected directly jumps to 40%. This discontinuity, just as the one in Fig. 2 (b), is a direct consequence of limited suspect testing.

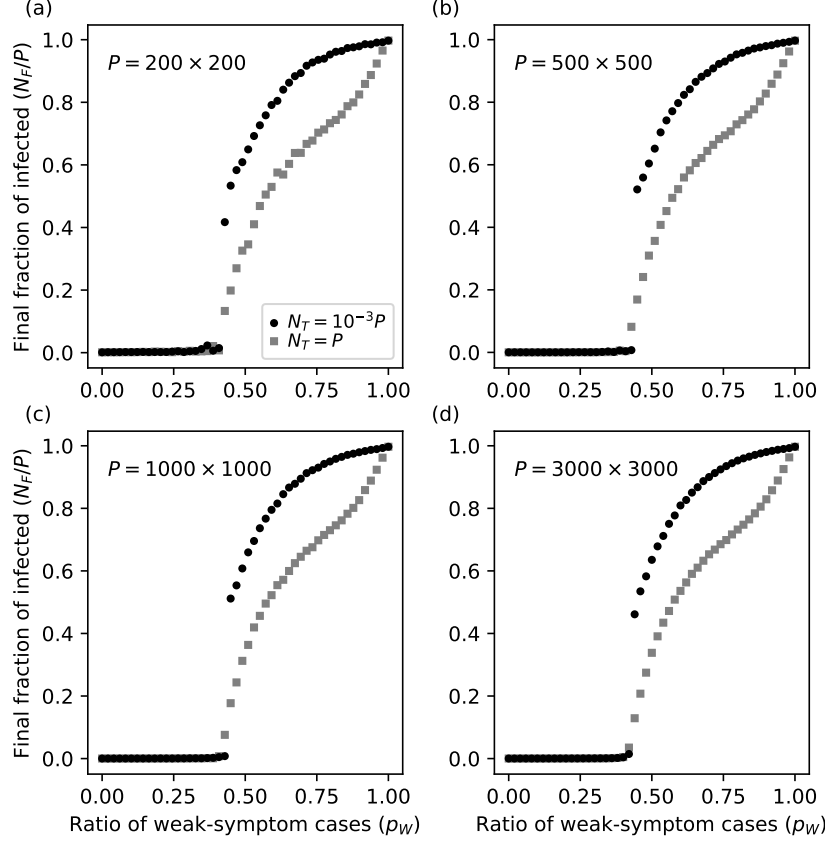


FIG. 4. Effect of the domain size on the transition for unlimited daily tests ( $N_T = P$ , gray dots) and limited daily tests ( $N_T = 10^{-3}P$ , black dots). The population for figures (a), (b), (c) and (d) is  $P = 200 \times 200$ ,  $P = 500 \times 500$ ,  $P = 1000 \times 1000$  and  $P = 3000 \times 3000$ , respectively. In all four cases the domain is initially seeded with  $4 \cdot 10^{-5}P$  randomly scattered weak-symptom cases.

To further illustrate the consequences of limited testing we consider three countries each with the same population size of 1 million and initially identical outbreaks. In all cases the disease starts to spread on day 0 and the outbreak is eventually detected on day 15. From day 15 all symptomatic cases are immediately quarantined, and they and their neighbours are tested with an upper limit of 1000 tests per day. After the identical start the countries' responses differ. The first country (blue in Fig. 5 (c)) reacts early and implements social distancing rules (e.g. masks compulsory in public places) on day 22. The other two countries only realize one week later that testing on its own is insufficient and at this point they implement the exact same SD rules as country one did seven days earlier. However, in country two and three (orange and red curves in Fig. 5 (c)) the number of infected continued to increase and the finite time horizon set by test limitations has passed. Unlike in country one, in countries two and three the combined containment effort fails.

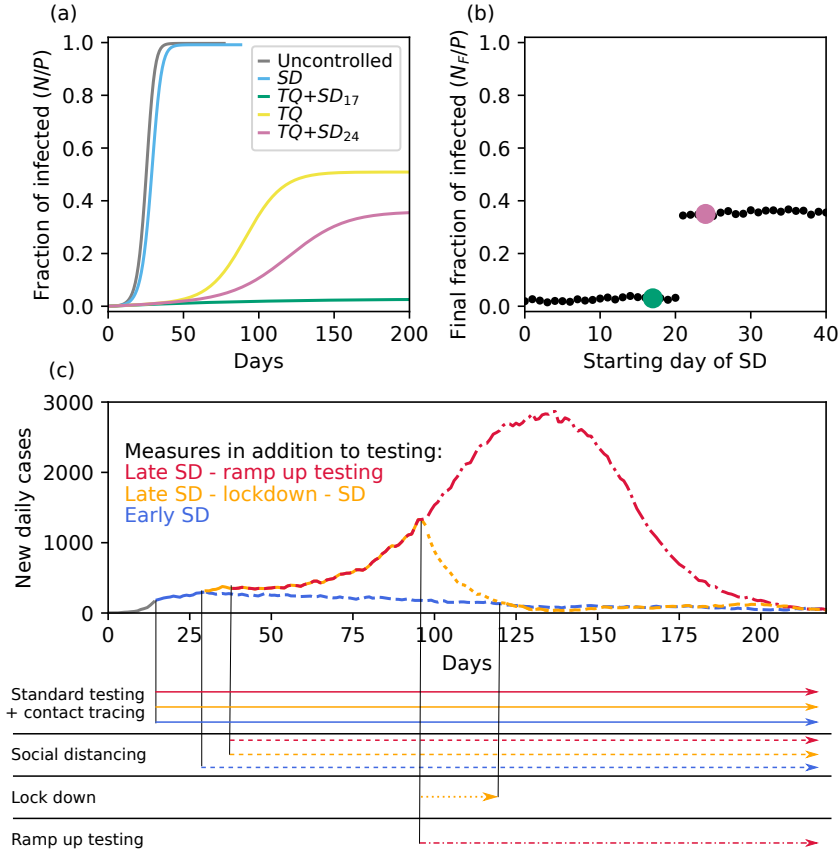


FIG. 5. Combined effect of quarantine and social distancing. (a) Comparison between different containment scenarios for  $p_W = 0.45$ , with testing and quarantining ( $TQ$ ) and social distancing ( $SD_n$ ) starting from day  $n$ . When social distancing, the transmission rate is reduced by 15%. Social distancing measures alone (blue and yellow curve) are mostly ineffective in comparison with combined quarantining and social distancing enforced from day 17. However, a late start of the latter results in a drastically higher percentage of final infected cases (pink curve). In all the  $TQ$  cases testing is limited to  $N_T = 10^{-3}P$ . (b) For  $p_W = 0.45$  and limited testing conditions ( $N_T = 10^{-3}P$ ) the combined effect of quarantining and early social distancing leads to a relatively low number of final infected cases if started early enough. A later start of  $SD$  results in an increasingly higher ratio of  $N_F/P$  up until a critical time is reached ( $t_{SD} = 21$ ) at which a discontinuous jump of  $N_F/P$  is observed. (c) Comparison between three different countries and their response under limited testing. A disease initially spreads undetected until day 15 (gray line). At this point all three countries implement contact tracing and quarantining of suspects. The first country implements  $SD$  early on day 22 and successfully manages to contain the outbreak (blue line). On the other hand, the other two countries wait implement  $SD$  one week later, however, their late action can not contain the disease spread and lead to a surge in new cases (yellow and red line). At day 97, one country decides to ramp up testing (additional 200 tests per day, red line), while the other resorts to a strict lock down (transmission probability reduced by 60%, yellow line).



Eventually, on day 97 country two and three impose additional measures. Country two increases test numbers by 200 every day (i.e. 20% of the original capacity). Despite the significant amount of new tests, the number of new daily cases continues to increase (red curve in Fig. 5 (c)). Country three on the other hand imposes a lock down. For lock down we assume that transmission rates decreases by 60%, the exact value is not important as long as it is sufficiently larger than the SD value. Once the numbers have considerably decreased on day 117 the yellow country goes back to the exact same SD measures and testing numbers that had failed on day 29. After the lock down and with a smaller number of active cases in the population, now these measures are effective and the number of daily cases decreases.

#### IV. DISCUSSION

The model suggestion that containment can be achieved if contact tracing is combined with an early implementation of social distancing is in line with the examples of South Korea, Japan, and Taiwan, where despite differences in contact tracing strategies (mobile phone data was used in South Korea but not in Japan), the common denominator of these cases is a high acceptance rate and immediate implementation of SD measures such as wearing masks. In contrast to many European states, these countries did not have to resort to full scale lock downs.

The longer term benefit of a lock down has been debated recently and for overwhelmingly large numbers of weak symptom carriers, lifting the lock down would indeed result in an immediate second outbreak as suggested by [18]. If however the disease is only moderately above the epidemic transition threshold (see estimates for COVID-19 parameters in Fig. 2 (b)), a lock down effectively acts as a reset shifting time to a stage before contact tracing is overwhelmed (i.e. to the left of the discontinuity in Fig. 5 (b)). Under such conditions, a subsequent combination of contact tracing and social distancing can keep the situation under control. The persistently low infection numbers in Hubei province as well as in countries like Austria and Germany where the lock down has been lifted more recently, indicate that COVID-19 may fall into this latter parameter regime.

#### V. CONCLUSIONS

Although the parameters of COVID-19 such as transmission rates and the percentage and role of weak-symptom carriers are still under debate, even for conservative estimates and with highly efficient contact tracing, including complete removal of local clusters, immediate quarantining and

unlimited testing in place, our models predict that containment fails. Nevertheless, testing is highly effective in limiting the spread, but under realistic conditions it will quickly reach its capacity limit. If additional social distancing measures are implemented before this happens the outbreak is contained, however if the implementation is just marginally late the identical combination of measures fails.

- 
- [1] M. Gandhi, D. S. Yokoe, and D. V. Havlir, “Asymptomatic transmission, the achilles’ heel of current strategies to control covid-19,” *N. Engl. J. Med.* **382**, 2158–2160 (2020).
- [2] N. W. Furukawa, J. T. Brooks, and J. Sobel, “Evidence Supporting Transmission of Severe Acute Respiratory Syndrome Coronavirus 2 While Presymptomatic or Asymptomatic,” *Emerg. Infect. Dis.* **26** (2020), 10.3201/eid2607.201595.
- [3] K. Mizumoto, K. Kagaya, A. Zarebski, and G. Chowell, “Estimating the asymptomatic proportion of coronavirus disease 2019 (COVID-19) cases on board the Diamond Princess cruise ship, Yokohama, Japan, 2020,” *Euro Surveill.* **25** (2020), 10.2807/1560-7917.ES.2020.25.10.2000180.
- [4] M. Day, “Covid-19: Four fifths of cases are asymptomatic, China figures indicate,” *BMJ* **369**, m1375 (2020).
- [5] M. M. Arons, K. M. Hatfield, S. C. Reddy, A. Kimball, A. James, Jessica R. Jacobs, J. Taylor, K. Spicer, A. C. Bardossy, L. P. Oakley, S. Tanwar, J. W. Dyal, J. Harney, Z. Chisty, J. M. Bell, M. Methner, P. Paul, C. M. Carlson, H. P. McLaughlin, N. Thornburg, S. Tong, A. Tamin, Y. Tao, A. Uehara, J. Harcourt, S. Clark, C. Brostrom-Smith, L. C. Page, M. Kay, J. Lewis, P. Montgomery, N. D. Stone, T. A. Clark, M. A. Honein, J. S. Duchin, and J. A. Jernigan, “Presymptomatic SARS-CoV-2 Infections and Transmission in a Skilled Nursing Facility,” *N. Engl. J. Med.* **382**, 2081–2090 (2020).
- [6] L. Zou, F. Ruan, M. Huang, L. Liang, H. Huang, Z. Hong, J. Yu, M. Kang, Y. Song, J. Xia, Q. Guo, T. Song, J. He, H. Yen, M. Peiris, and J. Wu, “SARS-CoV-2 Viral Load in Upper Respiratory Specimens of Infected Patients,” *N. Engl. J. Med.* **382**, 1177–1179 (2020).
- [7] V. Wong, D. Cooney, and Y. Bar-Yam, “Beyond Contact Tracing: Community-Based Early Detection for Ebola Response,” *PLOS Curr.* (2016), 10.1371/currents.outbreaks.322427f4c3cc2b9c1a5b3395e7d20894.
- [8] J. M. Kleinberg, “Navigation in a small world,” *Nature* **406**, 845–845 (2000).
- [9] A.-L. Barabási and R. Albert, “Emergence of Scaling in Random Networks,” *Science* **286**, 509–512 (1999).
- [10] Y. M. Bar-On, A. Flamholz, R. Phillips, and R. M., “Science Forum: SARS-CoV-2 (COVID-19) by the numbers,” *eLife* **9**, e57309 (2020).
- [11] G. Chowell, C. Castillo-Chavez, P. W. Fenimore, C. M. Kribs-Zaleta, L. Arriola, and J. M. Hyman, “Model Parameters and Outbreak Control for SARS,” *Emerg. Infect. Dis.* **10**, 1258–1263 (2004).

- [12] N. Petrosillo, G. Viceconte, O. Ergonul, G. Ippolito, and E. Petersen, “COVID-19, SARS and MERS: Are they closely related?” *Clin. Microbiol. Infect.* **26**, 729–734 (2020).
- [13] A. Khan, M. Naveed, M. Dur-e-Ahmad, and M. Imran, “Estimating the basic reproductive ratio for the Ebola outbreak in Liberia and Sierra Leone,” *Infect. Dis. Poverty* **4**, 13 (2015).
- [14] J. H. Kuhn and S. Bavari, “Asymptomatic Ebola virus infections—myth or reality?” *Lancet Infect. Dis.* **17**, 570–571 (2017).
- [15] P. Mbala, M. Baguelin, I. Ngay, A. Rosello, P. Mulembakani, N. Demiris, W. J. Edmunds, and J.-J. Muyembe, “Evaluating the frequency of asymptomatic Ebola virus infection,” *Phil. Trans. R. Soc. B* **372**, 20160303 (2017).
- [16] M. Roser, H. Ritchie, E. Ortiz-Ospina, and J. Hasell, “Coronavirus pandemic (covid-19),” Published online at OurWorldInData.org (2020), retrived from: <https://ourworldindata.org/coronavirus>.
- [17] A. A. Hagberg, D. A. Schult, and P. J. Swart, “Exploring network structure, dynamics, and function using networkx,” in *Proceedings of the 7th Python in Science Conference*, edited by G. Varoquaux, T. Vaught, and J. Millman (Pasadena, CA USA, 2008) pp. 11 – 15.
- [18] J. Giesecke, “The invisible pandemic,” *Lancet* **395**, e98 (2020).